Applied Catalysis A: General 381 (2010) 109–113

Contents lists available at ScienceDirect

Applied Catalysis A: General

journal homepage: www.elsevier.com/locate/apcata

Photocatalysis by Electron Transfer between Different-sized Anatases

Tsung-Ying Ke[a], Chi-Young Lee[a,b,*], Hsin-Tien Chiu[c]

[a] Department of Materials Science and Engineering, National Tsing Hua University, Hsinchu 30043, Taiwan, ROC
[b] Center for Nanotechnology, Materials Science, and Microsystems, National Tsing, Hua University, Hsinchu 30043, Taiwan, ROC
[c] Department of Applied Chemistry, National Chiao Tung University, Hsinchu 30050, Taiwan, ROC

ARTICLE INFO

Article history:
Received 5 January 2010
Received in revised form 19 March 2010
Accepted 24 March 2010
Available online 31 March 2010

Keywords:
Photocatalysis
Electron transfer
pH
P25

ABSTRACT

In the solution state, photocatalysis of micro- and nano-sized anatases can be optimized at flat band and in a high pH solution, respectively. Furthermore, a remarkable photocatalyst that can be adopted over a wide range of pH values was produced by mixing commercial micro- and nano-sized anatases. Mixing causes the electron transfer between the identical phase but different-sized TiO_2 particles, subsequently separating the electrons and holes, as well as greatly facilitating photocatalysis. As is well known, the commercially available photocatalyst P25, a mixture of anatase and rutile, achieves a superior photocatalytic performance from pH 3 to 10, owing to the electron transfer between the various phases. This study elucidates these mixed photocatalysts, P25 and mixture of micro and nano-sized anatases.

1. Introduction

TiO_2 has attracted considerable attention in recent decades, as evidenced by its numerous applications in photocatalysts, Li ion batteries, solar cells and biomaterials [1–5]. TiO_2 is the most studied photocatalyst owing to its high oxidation power of holes, excellent photo-stability, and low material cost. Composed of anatase and rutile phase TiO_2, Degussa P25 is a superior TiO_2 photocatalyst. As demonstrated elsewhere, the electron transfer between the TiO_2 phases enhances the photocatalysis performance [6]. Furthermore, in the water splitting of rutile-TiO_2/Pt electrodes [7], the electron transfer between the TiO_2 and Pt metal markedly raises the charge separation, subsequently reducing the charge recombination and significantly enhancing the photocatalytic performance. Recently, Grimes et al. reported that a $TiCl_4$ treated TiO_2 nanotube array markedly enhances solar cell performance [8]. A previous study postulated that the interaction between the nano-sized anatase particles produced by

$TiCl_4$ treatment and the TiO_2 nanotubes prolongs the lifetime of excited electrons, resulting in enhanced solar cell performance [9].

The above results demonstrate that the electron flow from a higher to a lower energy state leads to charge separation, subsequently reducing the charge recombination and prolonging the electron lifetime and, ultimately, enhancing the photocatalytic performance. Recent studies have introduced noble metals with low Fermi-level and high reduction affinity, e.g., Pt, Ni, Ag, into the photocatalytic system to remove electrons from catalysts, resulting in an improved performance [10,11]. Besides the use of intrinsically low Fermi-level materials, nano-particles with various band positions from their bulk materials are highly promising for use as an electron transfer medium.

This study investigated nano- and micro-sized anatases, along with their mechanical mixtures, in solutions with various pH values. The photocatalysis performances and band positions are also examined. The photocatalytic data of P25 are also provided for comparison with the results of our studies.

2. Experimental

2.1. Materials

Both micro- and nano-sized titanium dioxides are pure anatase phases. The former with a diameter range from tens of nanometers to several hundred nanometers were purchased from Sigma–Aldrich, and the latter with diameters of about 5 nanometers were purchased from Alfa Aesar. P25 type titanium dioxide with diameter of about 30 nanometers was purchased from Evonik Degussa. It consists mostly of anatase phase with some rutile phase. Pure Methylene Blue and Rhodamine B were purchased from Riedel-de Haen and Alfa Aesar respectively. All materials are used as received, except the rutile particles were obtained from P25 by dissolving the other phase, anatase, in HF solution and washing thoroughly with D.I. water.

* Corresponding author at: Department of Materials Science and Engineering, National Tsing Hua University, Hsinchu 30043, Taiwan, ROC.
E-mail address: cylee@mx.nthu.edu.tw (C.-Y. Lee).

0926-860X/$ – see front matter.
doi:10.1016/j.apcata.2010.03.052

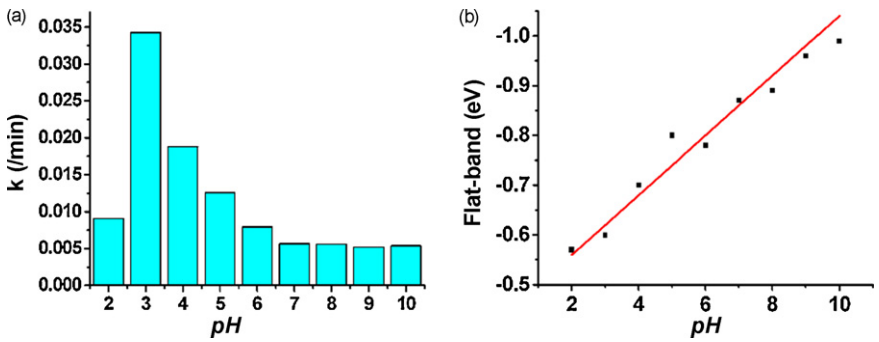

Fig. 1. (a) Calculated rate constants (k) and (b) the measured flat-band potentials of micro-sized anatase from pH 2 to 10.

2.2. Flat band

First, the working electrode is made by dispersing the test powders in D.I. water, spreading the gel on conducting substrates ITO by doctor-blade technique, and then drying at 373 K. The counter and reference electrodes are a platinum bar and Ag/AgCl respectively. The electrolyte is 1 M NaCl solution, and its pH is tuned to the desired values with NaOH and HCl solutions. The prepared electrodes are dipped in the electrolyte for 5 min before measuring. Between measurements, the electrodes are washed with D.I. water until the pH reaches the neutral state again.

The flat-band potentials are measured on a CHI 6081C electrochemical analyzer, and the experimental mode is impedance-potential. The measured frequency range is between 10 and 1000 Hz. Finally, the Mott–Schottky plots are made with the square of inverse capacity as ordinate and the corresponding voltage as abscissa. The flat-band potentials are determined by the intercepts with the abscissa.

2.3. Photocatalysis

For photocatalysis, the light source is a 180 W Xe bulb from Osram, and the temperature is controlled at 296 K by a water cooling jacket. Methylene Blue is the target pollutant, and Rhodamine B is also used in the micro-sized system to confirm the wide validity of our discussion. After mixing 0.01 g of powder with 50 mL of D.I. water and 30 mL of 0.6 mM Methylene Blue solution, we adjusted the pH with NaOH and HCl solutions. The pH value is measured with a Eutech pH 510 pH meter. After the stability of absorption has been reached, the solution is illuminated from the top under magnetic stirring. Samples of 0.5 ml are taken out every 3 min, filtered with 0.2 μm filter, and diluted with 2 ml of D.I. water, and the filtrate is analyzed to determine the dye concentration. A Hitachi UV–vis 3010 spectrophotometer is used to determine the dye concentration with the highest peaks in their spectra. According to a UV–vis study, the spectrum of the test pollutant, Methylene Blue, did not change with the pH. Therefore, the degradation of Methylene Blue primarily dominated the photocatalytic performance. For the mixing system, the mixing ratio between micro and nano-sized particles is 1:1 (0.005 g respectively). The results show a first-order behavior, so the pseudo-first-order rate constant, k, is calculated by the equation: $k = -[\ln(C/C_0)]/\Delta t$, where C is the final concentration, C_0 is the initial concentration, and Δt is the proceeding time. In addition, when Rhodamine B is used as the target pollutant, 0.04 g of powder is mixed with 32 mL of D.I. water and 8 mL of 1 mM Rhodamine B solution, and the sample interval is 10 min instead while other experimental details remain the same.

3. Results and discussion

Fig. 1a plots the photocatalytic performance of micro-sized anatase between pH 10 and 2 using the estimated pseudo-first-order reaction rate constant k. A decline of pH value from 10 to 2 increased k, with reached a maximum value at around pH 3

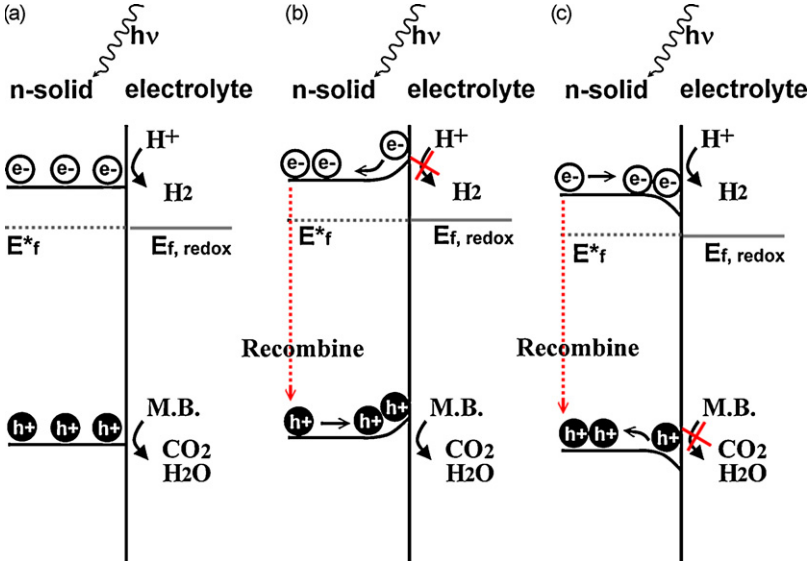

Fig. 2. Band structures of an n-type semiconductor with a (a) flat-band, (b) band-bending upwards, and (c) band-bending downwards in relationship with photocatalysis of methylene blue and reduction of hydronium.

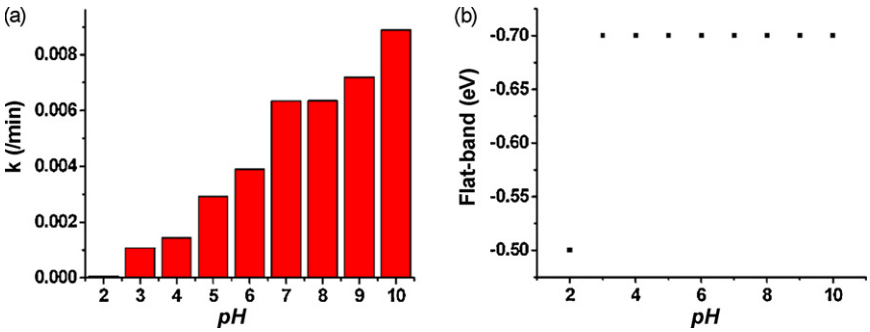

Fig. 3. (a) Calculated rate constants (k) and (b) the measured flat-band potentials of nano-sized anatase from pH 2 to 10.

and then fell sharply. In Fig. 1b, the flat-band potential, representing the band-edge positions determined from Mott–Schottky plots, decreased from −0.5 eV (referred to Ag/AgCl electrode) to −1.1 eV as the pH value increased from 2 to 10, which correlates with Nernst theory [12,13]. The performance of photocatalysis under varying pH environments did not correspond to their band-edge positions precisely.

Consider an n-type semiconductor in an aqueous solution. The band edge is commonly bent since electrons donate to the surface species, hydroxide and hydronium, until an equilibrium state is reached. Therefore, the pH value can be adjusted to shift the semiconductor band edge, which can be obtained by determining the flat-band potential from Mott–Schottky plots. Fig. 2 presents three possible scenarios. Fig. 2a indicates that when the band edge equals the intrinsic band position in a solid, the band is flat. An increasing pH value shifts the band-edge position negatively and then bends it upward (Fig. 2b), and vice versa (Fig. 2c). The band bending establishes an interior electric field which further influences the directions of the electron motions. As is well known, a large band bending of the semiconducting material drives electrons and holes to move in various directions, resulting in charge separation and leading to producing a good solar cell [14]. However, both the electrons and holes function at the interface in a photocatalytic reaction. Large band-bending drives either electrons or holes away from the interface, decelerating the reaction; whereas a flat-band condition accelerates the reaction.

Based on the above considerations, this study elucidates the photocatalytic behaviors of micro-sized anatase based on its interior electric field. Under most circumstances, for n-type semiconductors, the band bent upwards (Fig. 2b) and then generated an outwardly directed electric field, which tended to drive electrons to the interior and holes to the surface as they were generated by illumination. The holes functioning as an oxidizing reagent induced the decomposition of most pollutants. An electron generated by illumination, however, was driven away from the surface, subsequently preventing the formation of additional holes and ultimately limiting the photocatalytic reaction.

The electric field was reduced by reducing the pH value to shift down the band-edge potential, allowing electrons to approach near the surface. Accordingly, decreasing the pH value from pH 10 to 3 increased the reaction rate constant, k, especially in the range of acidic pH (Fig. 1a). At a pH value of around 3, the band flattened and both excitons impacted the catalytic reaction to optimize the reaction rates. Conversely, when the pH was 2 (Fig. 1), the band-edge potential shifted downwards further to around -0.6 eV, i.e. a value too close to the reduction potential of hydronium to overcome the reaction barrier, leading to a sharp decrease in k. Additionally, another pollutant, Rhodamine B, exhibited the same trend (Supporting information).

However, nano-sized anatase performed differently than micro-sized anatase. Fig. 3 plots the photodegradation rate constants and the flat-band potentials of nano-sized anatase respect to different pH values. Fig. 3a indicates that reaction rates decreased stepwise from pH 10 to 2. Fig. 3b reveals that nano-sized anatase retained its band position, −0.7 eV at pH 10–3; however, at a pH value of 2, the band position changed abruptly to −0.5 eV.

Generally, the photocatalytic reaction can be described as follows. Initially, under illumination, holes and electrons are produced simultaneously, and they reacted with OH^- and H^+ independently to form active species $OH^\bullet$ and $H^\bullet$, respectively, as shown in Eqs. (1) and (2). Thereafter, the active species $OH^\bullet$ and $H^\bullet$ decomposed pollutants.

$$OH^- + h^+ \rightarrow OH^\bullet \quad (1)$$

$$H^+ + e^- \rightarrow H^\bullet \quad (2)$$

The reaction rates of (1) and (2) determine the rate of photocatalytic reactions. Electrons and holes formed simultaneously should be consumed together. Otherwise, the remaining species inhibit further formation of electron and hole pairs. Previous studies normally introduced a scavenger to remove the slower one to accelerate the reaction [15,16]. In acid- and base-assisted catalytic reactions, H^+ and OH^- may function as electron and hole scavengers, respectively. Increasing the pH value increases the OH^- concentration, shifting reaction (1) to the right and accelerating hole consumption and ultimately improving the photocatalytic performance of a hole passive reaction. Conversely, decreasing the pH value enhances the photocatalytic performance of an electron passive reaction. Furthermore, increasing the pH value raises the $OH^-/OH^\bullet$ reduction potential, further facilitating the electron transfer (hole oxidation) and significantly enhancing photocatalytic performance.

For a catalyst, nano-sized anatase, that shows no band position change at pH 10–3, the increasing reaction rates with increasing pH values may be attributed to the rise in the $OH^-/OH^\bullet$ reduction potential to enhance activation of hole (Scheme 1). Experimental results indicate that the nano-sized anatase is effective in reduction reaction (as Eq. (2)) and is a significantly less active catalyst. However, at a pH value of 2, the potential difference between the band-edge position and the hydronium reduction potential is too small to induce reduction.

The above observations demonstrate that, with a decreasing pH value, increased oxidation efficiency of the holes improved the photocatalytic performance of micro-sized anatase. However, for nano-sized anatase, removal of the holes by increasing the OH^- concentration increases the reduction efficiency of electrons and enhances the photocatalytic performance. Whether a catalyst exists that is effective under various conditions is a priority concern. The fact that the two anatases differ in photocatalytic performances and flat-band potentials may allow them to couple with a synergistic effect via an electron transfer even over a wide range of pH.

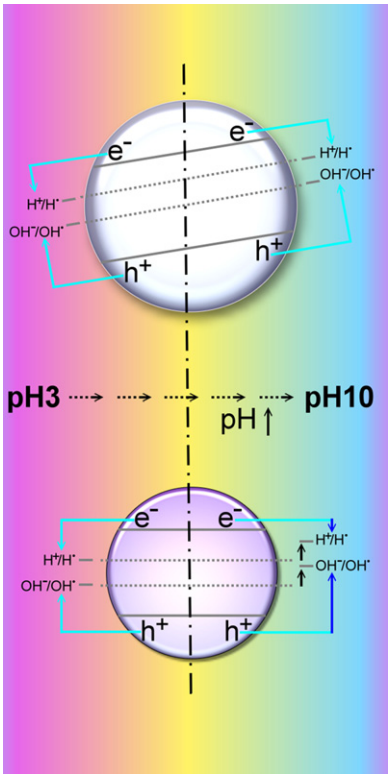

Scheme 1. The above and below spheres represent respectively the changes of the flat-band positions of micro- and nano-sized anatases from pH 3 to 10, with respect to the redox potentials of $H^+/H^\bullet$ and $OH^-/OH^\bullet$.

Fig. 4a shows the photocatalytic performance of the mixture of micro- and nano-sized anatases (in 50:50 ratio). The superior photocatalytic rates obtained from pH values 3–5 were approximate by equal to that of micro-sized anatase at pH3, as plotted in Fig. 2a. Synergy was evident even at a pH value of 9.

Fig. 4b shows the proposed synergy mechanism. The band-edge positions of micro-sized anatase are more negative than those of nano-sized anatase, thus facilitating the transfer of electrons from the former to the latter. Furthermore, the inter-particle attracting forces overwhelm other repelling forces [17], allowing the nano and micro-sized anatases to interact with each other, thus making the electron transfer a more efficient process. The fact that the photocatalytic reaction rate of micro-sized anatase at pH > 3 is limited by the passivation of electrons explains why the electron transfer to the large surface area electron activated nano-sized anatase significantly improves the photocatalytic reaction. Additionally, holes driven to the surface by upwardly bending bands can decompose pollutants efficiently.

At the pH value of 2, the conduction band potentials of nano-sized anatase are too low to reduce hydronium effectively, explaining why k was the sum of half of the individual values of k for the two forms of anatases.

As a mixture of wide range sized anatase and rutile [6], commercial P25 is effective in photocatalysis and solar cells. Therefore, this study also assessed the photocatalytic performance of P25 under various pH conditions (Fig. 4c). As expected, the k values closely approached those of the mixtures of micro and nano-sized anatases. Although synergy was observed again, the k value peaked at a pH value of 4, not 3.

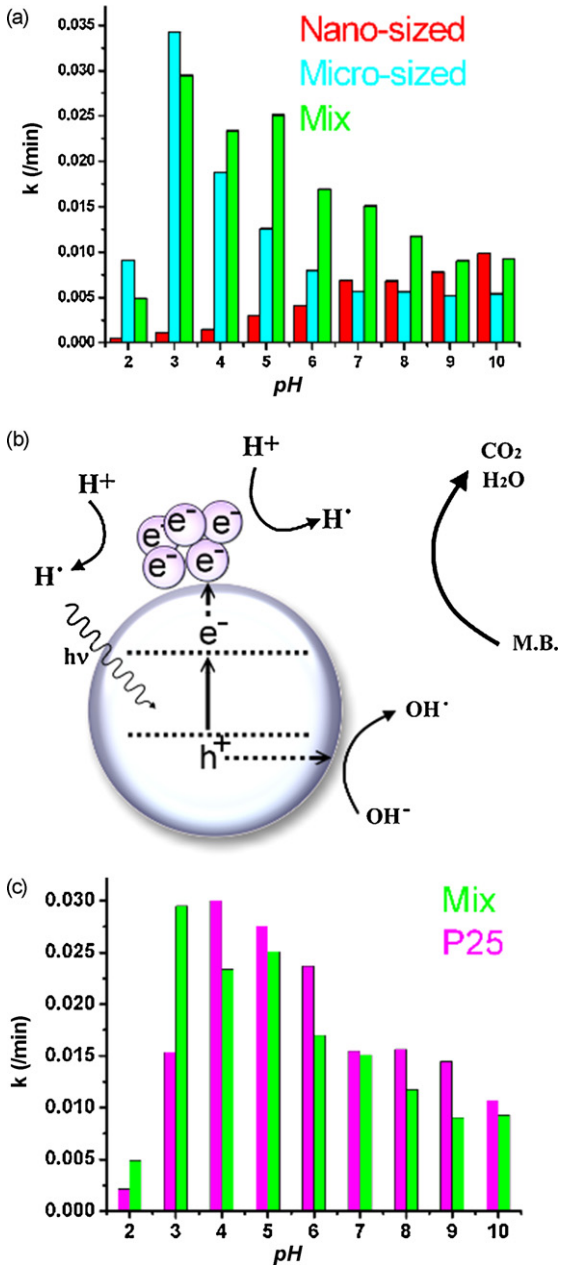

Fig. 4. (a) Calculated rate constants (k) of mixture, nano-, and micro-sized anatases from pH 2 to 10, (b) proposed synergism by electron transfer from micro to nano-sized anatases, and (c) calculated rate constants of P25 and mixture from pH 2 to 10. (Please note that the theoretical k values of the mix in (a) are the sum of half the individual values.)

4. Conclusions

In summary, band-edge position and the surrounding hydroxide concentration significantly influence the performance of a photocatalyst. The performance of micro-sized anatase can be optimized by reduced band bending owing to the population and utilization efficiencies of both holes and electrons. However, for nano-sized anatase in a solution with a high pH value, a high OH^- concentration forms massive active $OH^\bullet$ radicals, thus improving the photocatalytic performance significantly. Furthermore, an excellent photocatalyst for use over a wider range of pH values can be obtained by mixing the powders with various band positions. As a mixture of anatase and rutile titanium dioxides, commercial P25 exhibits great photocatalytic behavior. In this study, micro-

and nano-sized antases are mixed with different flat-band states to obtain an ascendent photocatalyst. Mixing the TiO^2 particles of different band positions facilitates their electron transfer, resulting in the separation of electrons and holes and ultimately improving the photocatalytic performance significantly.

Acknowledgment

The authors would like to thank the National Science Council of the Republic of China, Taiwan, for financially supporting this research under Contract No. NSC 96-2113-M-007-021.

Appendix A. Supplementary data

Supplementary data associated with this article can be found, in the online version, at doi:10.1016/j.apcata.2010.03.052.

References

[1] L.W. Zhang, H.B. Fu, Y.F. Zhu, Adv. Funct. Mater. 18 (2008) 2180–2189.
[2] Z.Y. Liu, D.D.L. Sun, P. Guo, J.O. Leckie, Nano Lett. 7 (2007) 1081–1085.
[3] T. Paunesku, T. Rajh, G. Wiederrecht, J. Maser, S. Vogt, N. StojicïEvicï, M. Proticï, B. Lai, J. Oryhon, M. Thurnauer, G. Woloschak, Nat. Mater. 2 (2003) 343–346.
[4] T. Paunesku, S. Vogt, B. Lai, J. Maser, N. StojicïEvicï, K.T. Thurn, C. Osipo, H. Liu, D. Legnini, Z. Wang, C. Lee, G.E. Woloschak, Nano Lett. 7 (2007) 596–601.
[5] X.W. Zhang, T. Zhang, D.D. Sun, Adv. Funct. Mater. 19 (2009) 3731–3736.
[6] T. Ohno, K. Tokieda, S. Higashida, M. Matsumura, Appl. Catal. A: Gen. 244 (2003) 383–391.
[7] A. Fujishima, K. Honda, Nature 238 (1972) 37–38.
[8] G.K. Mor, K. Shankar, M. Paulose, O.K. Varghese, C.A. Grimes, Nano Lett. 6 (2006) 215–218.
[9] P.R.F. Barnes, A.Y. Anderson, S.E. Koops, J.R. Durrant, B.C.J. O'Regan, J. Phys. Chem. C 113 (2009) 1126–1136.
[10] Y.C. Chiou, U. Kumar, J.C.S. Wu, Appl. Catal. A: Gen. 357 (2009) 73–78.
[11] M. Hara, J. Nunoshige, T. Takata, J.N. Kondo, K. Domen, Chem. Commun. (2003) 3000–3001.
[12] D.W. Chen, A.K. Ray, Chem. Eng. Sci. 56 (2001) 1561–1570.
[13] U. Kolle, J. Moser, M. Gratzel, Inorg. Chem. 24 (1985) 2253–2258.
[14] B. O'regan, M. Gratzel, Nature 353 (1991) 737–740.
[15] J.L. Ferry, W.H. Glaze, Langmuir 14 (1998) 3551–3555.
[16] J.M. Monteagudo, A. Dura'n, Chemosphere 65 (2006) 1242–1248.
[17] For metal–oxide particles in aqueous solutions, there are three main inter-particle forces: van der Waals force, hydrogen bonding, and electrostatic force. The former two are always attractive. On the other hand, the electrostatic force depending on the surface charge of the particles can be attractive or repulsive. To examine the particle interaction, we used two micro-sized anatases with a point of zero zeta potential (PZZP) at pH 3 (designated M3) and pH 6 (designated M6) and a nano-sized anatase (PZZP—pH 6.5, designated N). In pH 3–6, both M6 and N with positive surface charge repel each other by electrostatic force; on the contrary, M3 with negative charge attracts positively charged N. According to the photocatalysis performances, both of the mixtures of M3 with N and M6 with N, the enhanced performances were obtained in spite of the electrostatic force, implying that in both cases, rigid inter-particle bonding exists. In short, the attraction of van der Waals force and hydrogen bond overwhelmed the repulsion of electrostatic force, dominating the interaction, and contributing the inter-particle bonding.